

Computational Modeling of Blood Flow in a Non-Uniform Circular Tube under Magnetic Field effects with Application to Pulmonary Edema Disease

Vishakha Gupta¹, Meenu Chawla², Anil Kumar³, Pooja Khurana⁴, Akash⁵, Bajarang Prasad Mishra⁶

¹Department of Mathematics, Dyal Singh College, Karnal, Haryana, India. Email: vi_shu85@yahoo.co.in

²Department of Mathematics, J.C. Bose University of Science and Technology (YMCA), Sector-6 Mathura Road, Faridabad, Haryana, India 121006. Email: meenuchawla@jcboseust.ac.in (Corresponding Author)

³Department of Applied Sciences and Humanities, IMS Engineering College, Ghaziabad- 201009, UP, India. Email: dranilkumar73@rediffmail.com

⁴Department of Applied Sciences, School of Engineering and Technology, Manav Rachna International Institute of Research and Studies, Sector 43, Surajkund Road, Faridabad, Haryana 121004. Email: pooja.fet@mriu.edu.in

⁵Department of Mathematics, South Point Degree College, Ratangarh, Gohana Road, Sonapat, Haryana 131022. Email: southpoint9@gmail.com

⁶Department of Electronics and Communication Engineering, Graphic Era (Deemed to Be) University, Dehradun, Uttarakhand, India. Email: bpmishra.ece@geu.ac.in

*Corresponding author: Dr. Meenu Chawla, Department of Mathematics, J.C. Bose University of Science and Technology (YMCA), Sector-6 Mathura Road, Faridabad, Haryana, India 121006. Email: meenuchawla@jcboseust.ac.in

ABSTRACT

We conduct a computational modeling analysis of blood flow in a non-uniform circular tube with the presence of an external magnetic field: Application to pulmonary edema disease. Blood is modeled as an incompressible, viscous and electrically conducting fluid flowing through an axially non-uniform circular tube that mimics physiological aberration in pulmonary arteries. Equation describing the state of MHD blood flow is derived in terms of the continuity and Navier–Stokes equations with magnetic field effects incorporated through Hartmann number. The computational study focuses on the effect of different magnetic field strengths, tube geometric features, and flow characteristics on velocity distribution, pressure gradient, wall shear stress, and volumetric flow rate. Adequate computational methods are adopted to perform the numerical simulations of hemodynamic behaviors in normal and diseased states. A considerable decrease in axial velocity accompanied with attenuation of flow disturbances of the fluid is indicated by an increase in Hartmann number, which results from a resistive Lorentz force generated by the magnetic field. In addition, non-uniform artery geometries change the pressure and increase hydraulic resistance which is specific to pulmonary edema.

Keywords: Pulmonary edema, mathematical model, blood flow, simulations, flow parameter, viscosity coefficient.

Mathematical Subject Classification [MSC 2020]: 76B75, 76D55, 76N25

How to cite this article: Gupta V, Chawla M, Kumar A, Khurana P, Akash, Mishra BP. Computational Modeling of Blood Flow in a Non-Uniform Circular Tube under Magnetic Field effects with Application to Pulmonary Edema Disease. Int J Drug Deliv Technol. 2026;16(60s):27-37. DOI: 10.25258/ijddt.16.60s.4

Source of support: Nil.

Conflict of interest: None

1. INTRODUCTION

An understanding of blood flow dynamics, particularly in the context of pulmonary edema, necessitates advanced computational modeling of blood flow through non-uniform circular tubes under the influence of magnetic fields. Magnetic Resonance Imaging (MRI) combined with Arterial Spin Labeling (ASL) serves as a non-invasive technique for investigating pulmonary

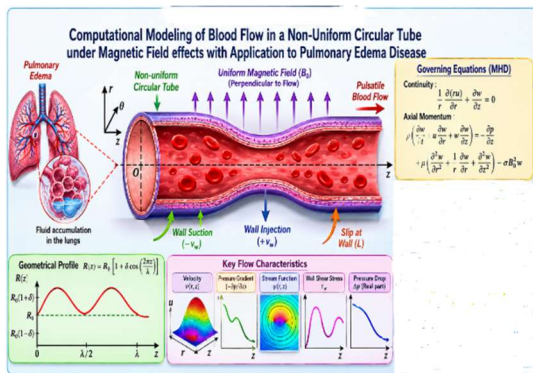
blood flow dynamics. This method facilitates the visualization of fundamental vascular regulatory mechanisms and enables the detection of dynamic interactions among different blood flow regions within the lungs. Previous studies have demonstrated that nonlinear prediction techniques can effectively characterize the temporal and spatial behavior of pulmonary blood flow. Such computational and imaging approaches provide valuable insights into a wide range of physiological and pathological conditions,

including pulmonary edema, thereby enhancing our understanding of disease progression, hemodynamic alterations, and vascular function. Because anomalies in blood circulation are intimately linked to a number of cardiovascular and pulmonary disorders, blood flow via arteries is a significant field of study in biomechanics and biomedical engineering. The physiological function of the circulatory system can be better understood by mathematical and computational modeling of blood flow, which also aids in comprehending the mechanics underlying a number of clinical disorders. Magnetohydrodynamic (MHD) and computational fluid dynamics (CFD) techniques have been widely used in recent years to study blood flow characteristics in diseased arteries and blood vessels with intricate geometries. Because red blood cells include hemoglobin, which contains iron, and ions, blood is regarded as an electrically conducting fluid. As a result, applying an external magnetic field has a big impact on how blood flows. A Lorentz force is created when the magnetic field and conducting blood interact. This force opposes fluid travel and modifies the artery's velocity distribution, wall shear stress, and pressure gradient. Medical science can benefit greatly from this phenomena, especially in the areas of magnetic medication targeting, blood flow modulation, treating hyperthermia, and cardiovascular diagnostics. Hemodynamic properties are also significantly influenced by the geometry of blood vessels. Many physiological conditions result in non-uniform arteries because of stenosis, constrictions, or enlargement brought on by the advancement of a disease. These changes in artery geometry increase blood circulation resistance and disrupt the regular flow pattern. Therefore, computational analysis of blood flow in non-uniform circular tubes is crucial to comprehending the emergence of pulmonary problems and cardiovascular illnesses.

Fig 1 Geometrical Function of Blood flow in pulmonary edema

A dangerous medical disease known as pulmonary edema is defined by the buildup of extra fluid in the lungs, which impairs oxygen exchange and raises pulmonary vascular resistance. Pulmonary artery pressure and flow dynamics are impacted by the changed blood circulation linked to pulmonary edema. Therefore, research on blood flow in non-uniform arteries under magnetic field effects can yield important insights into the hemodynamic alterations that take place during this illness. Comprehending these impacts could lead to better treatment approaches and biological uses of magnetic field-assisted therapies. Numerous researchers have used analytical and numerical techniques to study MHD blood flow in stenosed and tapered arteries. Research has demonstrated that the flow behavior and distribution of wall shear stress are greatly influenced by the Hartmann number, Reynolds number, and vessel geometry. The combined effects of magnetic fields and non-uniform circular tube geometry in connection to pulmonary edema disease, however, have not received much attention. Through numerical analysis and computational modeling, the current study seeks to close this gap. Blood is represented in this study as an electrically conducting, viscous, and incompressible fluid that flows through a non-uniform circular tube while being affected by an external magnetic field. The Navier-Stokes equations with MHD effects and the continuity equation are used to create the governing equations. The impacts of flow parameters, tube geometry, and magnetic field strength on velocity profiles, pressure distribution, and wall shear stress are examined by numerical simulations. The results of this study could be beneficial for clinical research, biomedical engineering, and the comprehension of hemodynamics associated with pulmonary edema. Womersley [1, 2] investigated oscillatory flow in cylindrical tubes with uniform cross-sections.

Saket and Kumar [3] studied blood flow via a stenosed artery with a porous effect by modeling blood as a Newtonian fluid. Bitoun and Bellet [6] looked at the relationship between pulsatile blood flow and microcirculation stenosis. The analysis of blood flow in elastic arteries and its applications are studied by Schneck and Ostrach



[5] and Kumar et al. [4]. In each of these studies, the tube walls were assumed to be impermeable.

However, in small blood vessels, the magnetization of the vessel wall becomes a critical factor. Manton [7] studied flow in progressively expanding axisymmetric tubes with low Reynolds numbers. Pulsatile blood flow in circular tubes with varying cross-sections under suction and injection conditions was investigated by Radhakrishnamacharya et al. [8] and Prasad et al. [9]. Since blood exhibits observable non-Newtonian behavior at low shear rates and the shear rate is usually low downstream of a stenosis, it is crucial to incorporate blood's non-Newtonian characteristics in these flow assessments. Following research by Chow [10], Hill and Bedford [11], and Srivastava and Agarwal [12], scientists have become more interested in blood, which is a suspension of cells and plasma.

Nakayama and Sawada [13] studied the flow of a non-Newtonian fluid through an axisymmetric stenosis numerically. Elnaby et al. [14] investigated the pulsatile flow of a non-Newtonian biviscous fluid in a tube with impermeable walls and a changeable cross-section under the effect of an external magnetic field. Sanyal et al. [15] examined the pulsatile flow of a biviscous fluid under suction and injection in a tube with a changing cross-section. In stenotic arteries with little stenosis, Kumar and Agarwal [16] found that stenosis geometry affected flow fields and metrics such wall shear stress. Galerkin techniques and the finite element methodology were also used by Sharma et al. [18] in their study of an MHD flow in a stenosis artery. Kumar (19) conducted a mathematical analysis of blood flow in a circular tube with a changeable cross-section, accounting for a non-Newtonian biviscous incompressible fluid and a permeable wall. Kumar and Agrawal (20) provided a computer analysis of blood flow via elastic arteries that accounts for porous wall effects. Kumar and Agarwal's computer model was used to investigate the hydrodynamic characteristics of blood flow via a stenotic artery (21). Gupta (22) investigated the application of a finite element Galerkin algorithm to simulate blood flow in arteries under magnetic influence. Gupta (23) examined the carotid artery's blood flow. Kumar (24) proposed a performance model and investigation of blood flow in small vessels with consideration for magnetic influences. The impact of permeability on blood flow in a stenosed artery

was numerically investigated by Kumar et al. (25) using the Crank-Nicolson method. In order to forecast and evaluate blood flow in stenosed arteries, Kumar et al. (26) employed magnetization and permeability parameters. With particular reference to pulmonary edema disease, the main goal of this work is to examine the pulsatile flow of blood through a non-uniform circular tube under the effect of an external magnetic field. To replicate realistic physiological flow conditions, the model takes into account the effects of magnetic forces and slip velocity at the artery wall. Blood is viewed as an electrically conducting, viscous, and incompressible fluid passing through a tube with a variable cross-section that symbolizes anomalies in the pulmonary arteries linked to fluid buildup and vascular obstruction during pulmonary edema.

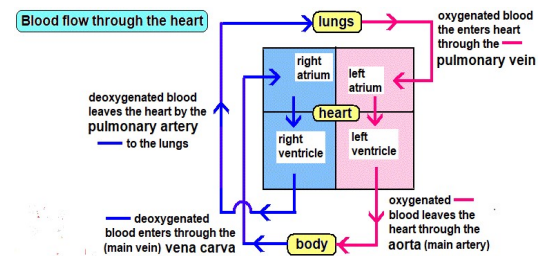


Fig 2 Geometrical Heart Function of Blood flow in pulmonary edema The Navier-Stokes and continuity equations are used to create the governing equations that describe the magnetohydrodynamic (MHD) blood flow. The velocity distribution, pressure gradient, flow rate, and wall shear stress are all roughly analytically solved using the perturbation technique. The impact of the Hartmann number, which describes the strength of the applied magnetic field and how it interacts with the electrically conducting blood, is given special consideration. By lowering axial velocity and minimizing flow disruptions brought on by the resistive Lorentz force, the computational analysis shows that magnetic field effects considerably alter the pulsatile flow behavior. Additionally, the existence of wall slip and varied arterial geometry modifies the hemodynamic properties and affects the blood flow resistance. These results are especially pertinent to pulmonary edema, where aberrant pressure fluctuations and poor pulmonary circulation impact cardiovascular and oxygen delivery. The computational modeling of pulsatile blood flow via a non-uniform circular tube exposed to an external magnetic field, with application to pulmonary edema disease, is the

basis of the current study's geometric structure. The physiological activity of pulmonary arteries impacted by vascular anomalies and fluid buildup is represented by the tube geometry. To replicate the non-uniform arterial circumstances found in sick pulmonary circulation, the tube's radius changes along the axial direction. The axial direction of blood flow is indicated by z and the radial coordinate by r in a cylindrical coordinate system (r, θ, z) . By using a mathematical model of the artery's shape as a sinusoidally fluctuating circular tube, flow disruptions, pressure variations, and wall shear stress under pathological conditions can be investigated. The governing equations take into account the magnetohydrodynamic effects that arise when an external magnetic field is applied perpendicular to the direction of blood flow. The model's physiological relevance for pulmonary edema analysis is further increased by the addition of wall slide, suction, and injection settings. Consequently, the current computer study of MHD blood flow in a changeable circular tube offers important new information about the intricate dynamics of blood circulation in illness. The research could advance our knowledge of the hemodynamics associated with pulmonary edema and help create better diagnostic and therapeutic approaches as well as biological uses of magnetic field-assisted treatment. This article provides valuable insights into the application of magnetic field effects on blood flow and their potential utilization in biomedical settings. The findings contribute to a better understanding of cardiovascular complications associated with pulmonary edema. The proposed computational model offers a useful framework for future investigations in medical diagnosis, treatment planning, and biofluid engineering research. Furthermore, the study highlights the significance of magnetohydrodynamic effects in regulating blood flow characteristics, which may assist in the development of advanced therapeutic strategies for cardiovascular disorders.

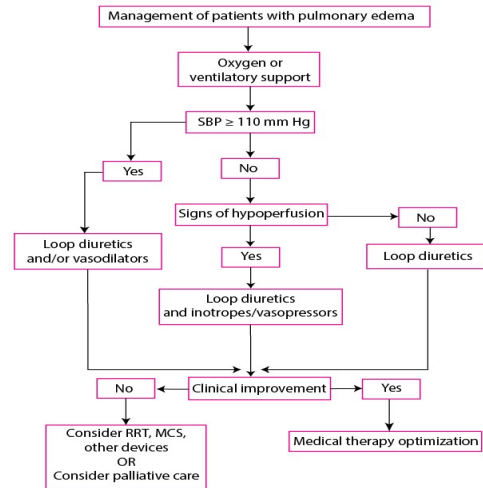


Fig 3 Algorithmic function of blood flow in artery in presence of pulmonary edema
2. Formulation of the Problem

The current work examines the pulsatile blood flow via a non-uniform circular tube while an external magnetic field is present, with a focus on pulmonary edema. It is believed that blood is a viscous, electrically conducting, incompressible fluid passing through a cylindrical tube with a changeable radius. The pulmonary arteries' physiological irregularities brought on by fluid buildup and vascular abnormalities linked to pulmonary edema are represented by the tube's non-uniform geometry.

A cylindrical coordinate system (r, θ, z) is examined, in which the radial direction is represented by r - and the z -axis is taken along the tube's axis. All physical quantities are assumed to be independent of the angular coordinate θ due to axisymmetric flow. Perpendicular to the direction of blood flow, an external uniform magnetic field B_0 is applied. Assuming low magnetic strength, the induced magnetic field is disregarded. number of Reynolds

The radius of the non-uniform circular tube is represented as

$$R(z) = R_0 \left\{ 1 + \epsilon S \left(\frac{\epsilon z}{R_0} \right) \right\} \text{ with } S(0) = 1, \quad (1)$$

Computational Modeling of Blood Flow in a Non-Uniform Circular Tube under Magnetic Field effects with Application to Pulmonary Edema Disease

Here, $\varepsilon = \frac{R_0}{L} (\ll 1)$ denotes the tube wall slope parameter, L is the characteristic length of the tube, and R_0 represents the tube radius at the inlet $z=0$.

The governing equation are given by

$$\frac{1}{r} \frac{\partial}{\partial r} (ru) + \frac{\partial w}{\partial z} = 0$$

(2)

$$\frac{\partial u}{\partial t} + u \frac{\partial u}{\partial r} + w \frac{\partial u}{\partial z} = -\frac{1}{\rho} \frac{\partial P}{\partial r} + \nu_B (1+b^{-1}) \left[\frac{1}{r} \frac{\partial}{\partial r} \left(r \frac{\partial u}{\partial r} \right) \frac{\delta y}{\delta x} \frac{\delta y}{\delta x} + \frac{\partial^2 u}{\partial z^2} \right]$$

(3)

$$\frac{\partial w}{\partial t} + u \frac{\partial w}{\partial r} + w \frac{\partial w}{\partial z} = -\frac{1}{\rho} \frac{\partial P}{\partial z} + \nu_B (1+b^{-1}) \left[\frac{1}{r} \frac{\partial}{\partial r} \left(r \frac{\partial w}{\partial r} \right) + \frac{\partial^2 w}{\partial z^2} - M w \right]$$

(4)

where u and w are the velocity components in $(r, 0, z)$ axes, t the time, P is the pressure, ν_B the kinematic coefficient of viscosity, ρ the fluid density and b the upper limit of the apparent viscosity coefficient, H is the Hartmann number. The normal component of the fluid velocity at the tube wall is given by

$$u - \frac{dR}{dz} w = v_s (1 + \delta e^{int}) \left\{ 1 + \left(\frac{dR}{dz} \right)^2 \right\}^{\frac{1}{2}} \text{ at } r = R(z),$$

(5)

where v_s is the steady state suction/injection velocity, δ is the ratio of the amplitudes of the oscillatory and steady parts of the suction/injection velocity and n is the frequency of the oscillation.

The important dimensionless parameter appearing in the analysis is the Hartmann number defined by

$$M = B_0 R_0 \sqrt{\frac{\sigma}{\mu}}$$

which measures the relative influence of magnetic forces to viscous forces in the blood flow.

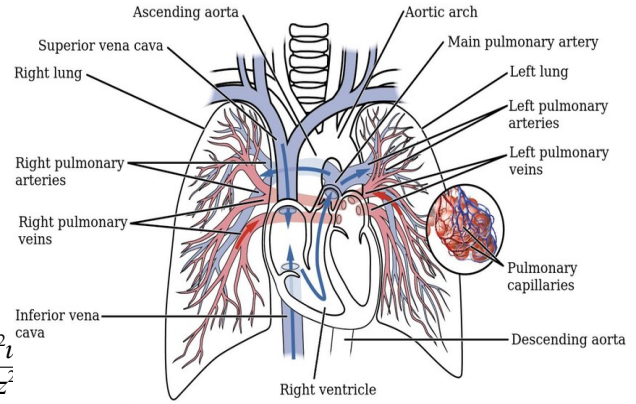


Fig. 4. Flow diagram of blood flow through artery in presence of pulmonary edema

On the boundary, the flow satisfies a slip condition.

$$w + \frac{dR}{dz} u = u_0 \text{ at } r = R(z)$$

(6)

i.e. the tangential velocity is non-zero at the wall, where u_0 is the slip parameter. The axisymmetric of the flow gives

$$\frac{\partial w}{\partial r} = 0, u=0 \text{ at } r=0.$$

(7)

Again the flux at the initial cross-section (i.e. $z=0$) is assumed to be in phase with the suction/injection velocity and is taken as

$$Q = Q_s (1 + \delta e^{int}) \text{ at } z=0,$$

(8)

where Q_s is the steady state flux at the initial cross-section. We introduce stream function $\Psi(r, z)$ by

$$u = -\frac{1}{r} \frac{\partial \Psi}{\partial z} \text{ and } w = \frac{1}{r} \frac{\partial \Psi}{\partial r}.$$

(9)

Eliminating P (i.e. pressure) from (3) and (4) and using (9), we get

$$\frac{\partial \Omega}{\partial t} + \left\{ \frac{\partial \Psi}{\partial r} \frac{\partial}{\partial z} \left(\frac{\Omega}{r} \right) - \frac{\partial \Psi}{\partial z} \frac{\partial}{\partial r} \left(\frac{\Omega}{r} \right) \right\} = \nu_B (1+b^{-1}) \left\{ \frac{\partial^2 \Omega}{\partial z^2} + \frac{\partial}{\partial r} \left(\frac{1}{r} \frac{\partial}{\partial r} (r \Omega) \right) - M \Omega \right\},$$

(10)

where

$$\Omega = \frac{\partial}{\partial r} \left(\frac{1}{r} \frac{\partial \Psi}{\partial r} \right) + \frac{\partial}{\partial z} \left(\frac{1}{r} \frac{\partial \Psi}{\partial z} \right).$$

(11)

The boundary conditions (6) and (7) in terms of Ψ can be written as

$$\left. \begin{aligned} \frac{\partial \Psi}{\partial r} - \frac{dR}{dz} \frac{\partial \Psi}{\partial z} &= ru_0 \text{ at } r = R(z) \\ \Psi &= 0, \frac{1}{r} \frac{\partial \Psi}{\partial z} = 0, \frac{\partial}{\partial r} \left(\frac{1}{r} \frac{\partial \Psi}{\partial r} \right) = 0 \text{ as } r \rightarrow 0 \end{aligned} \right\}$$

(12)

Combining the continuity equation (2) with boundary conditions (5) and (8) for axisymmetric flow yields:

$$\Psi = \frac{1}{2\pi} (1 + \delta e^{\text{int} + K}) \left[Q_s - 2\pi v_s \int_0^z R(\xi) \left\{ 1 + \left(\frac{dR}{d\xi} \right)^2 \right\}^{\frac{1}{2}} d\xi \right] \text{ at } r = R(z). \quad (13)$$

The non-dimensional variables are defined as follows:

$$z' = \frac{\varepsilon z}{R_0}, \quad r' = \frac{r}{R_0}, \quad t' = nt, \quad \Psi' = \frac{2\pi \Psi}{Q_s}, \quad \omega = 2\pi R_0^3 \frac{\Omega}{Q} \text{ (i.e. } \delta \approx \frac{\delta z \pi R_0^3 \Omega}{Q} \text{ order } \delta^2 \text{).} \quad (14)$$

and

$$R_e = \frac{Q_s}{2\pi \nu_B R_0}, \quad \alpha^2 = \frac{n R_0^2}{\nu_B}, \quad v_s' = \frac{2\pi R_0^2}{\varepsilon Q_s} v_s \quad (15)$$

Equations (10) and (11), together with boundary conditions (12) and (13), can be expressed in non-dimensional form (after dropping the primes) as:

$$\alpha^2 \frac{\partial \omega}{\partial t} + \varepsilon R_e \left\{ \frac{1}{r} \frac{\partial \omega}{\partial r} \frac{\partial \omega}{\partial z} - \frac{\partial \omega}{\partial z} \frac{\partial}{\partial r} \left(\frac{\omega}{r} \right) \right\} = (1 + b^{-1}) \left\{ \varepsilon^2 \frac{\partial^2 \omega}{\partial z^2} + \frac{\partial^2 \omega}{\partial r^2} + \frac{1}{r} \frac{\partial \omega}{\partial r} - \frac{\omega}{r^2} - M\omega \right\}, \quad (16)$$

$$\omega = \frac{1}{r} \left(\frac{\partial^2 \Psi}{\partial r^2} - \frac{1}{r} \frac{\partial \Psi}{\partial r} + \varepsilon^2 \frac{\partial^2 \Psi}{\partial z^2} \right), \quad (17)$$

$$\left. \begin{aligned} \frac{\partial \Psi}{\partial r} - \varepsilon^2 \frac{dS}{dz} \frac{\partial \Psi}{\partial z} &= ru_0, \\ \Psi &= (1 + \delta e^{\text{int} + K}) \left[1 - v_s \int_0^z G(\xi) d\xi \right] \end{aligned} \right\} \text{ at } r = S(z), \quad (18)$$

$$\Psi = 0, \quad \frac{\partial \Psi}{\partial z} = 0, \quad \frac{\partial}{\partial r} \left(\frac{1}{r} \frac{\partial \Psi}{\partial r} \right) = 0 \text{ as } r \rightarrow 0, \quad (19)$$

where R_e is the Reynolds number of entrance flow, α is Womersley parameter, v_s is the leakage parameter and

$$G(z) = S(z) \left\{ 1 + \varepsilon^2 \left(\frac{dS}{dz} \right)^2 \right\}^{\frac{1}{2}}.$$

In equation (18), it can be noted that $\delta = 0$ and $v_s = 0$ indicates the steady flow and the impermeability of the tube wall respectively.

The perturbation technique is used by treating the non-uniformity parameter as a small quantity in order to achieve analytical solutions. For various Hartmann number and slip parameter values, approximate formulae for velocity distribution, pressure gradient, and volumetric flow rate are generated and computationally examined. The hemodynamic features linked to pulmonary edema disease under magnetic field impacts are investigated using the acquired results.

3. Computational Method

We assume the pulsatile flow comprises a steady component and a small-amplitude oscillatory component, allowing us to neglect terms

of order δ^2 . With this approximation we seek solutions to equations (16)–(19) in the form:

$$\left. \begin{aligned} \omega &= (\omega_{00} + \delta e^{it} \omega_{01}) + \varepsilon (\omega_{10} + \delta e^{it} \omega_{11}) + o(\varepsilon^2, \delta^2), \\ \Psi &= (\Psi_{00} + \delta e^{it} \Psi_{01}) + \varepsilon (\Psi_{10} + \delta e^{it} \Psi_{11}) + o(\varepsilon^2, \delta^2) \end{aligned} \right\} \quad (20)$$

Substituting the perturbation expansion (20) into equations (16)–(19), ω and Ψ collecting terms of equal powers in ε , we obtain the following equations and boundary conditions:

(i) Zeroth order steady part:

$$D^2 \omega_{00} = 0,$$

$$\omega_{00} = \frac{\partial}{\partial r} \left(\frac{1}{r} \frac{\partial \Psi_{00}}{\partial r} \right),$$

$$\frac{\partial \Psi_{00}}{\partial r} = ru_0, \quad \Psi_{00} = 1 - v_s F(z) \text{ at } r = S(z), \quad (21c)$$

$$\Psi_{00} = 0, \quad \frac{\partial \Psi_{00}}{\partial z} = 0, \quad \frac{\partial}{\partial r} \left(\frac{1}{r} \frac{\partial \Psi_{00}}{\partial r} \right) = 0 \text{ as } r \rightarrow 0, \quad (21d)$$

where $D^2 \equiv \frac{\partial^2}{\partial r^2} + \frac{1}{r} \frac{\partial}{\partial r} - \frac{1}{r^2}$ and $F(z) = \int_0^z S(\xi) d\xi$

(i) Zeros order oscillatory part:

$$D^2 \omega_{01} = \alpha_1^2 \omega_{01}, \quad (22a)$$

$$\omega_{01} = \frac{\partial}{\partial r} \left(\frac{1}{r} \frac{\partial \Psi_{01}}{\partial r} \right), \quad (22b)$$

$$\frac{\partial \psi_{01}}{\partial r} = 0, \psi_{01} = 1 - \nu_s F(z) \text{ at } r = S(z),$$

(22c)

$$\psi_{01} = 0, \frac{\partial \psi_{01}}{\partial z} = 0, \frac{\partial}{\partial r} \left(\frac{1}{r} \frac{\partial \psi_{01}}{\partial r} \right) = 0 \text{ as } r \rightarrow 0,$$

(22d)

$$\text{where } \alpha_1 = \frac{\sqrt{i\alpha^2}}{1+b^{-1}}.$$

(ii) First order steady part:

$$D^2 \omega_{10} = R_{e1} \left\{ \frac{1}{r} \frac{\partial \psi_{00}}{\partial r} \frac{\partial \omega_{00}}{\partial z} - \frac{\partial \psi_{00}}{\partial z} \frac{\partial}{\partial r} \left(\frac{\omega_{00}}{r} \right) \right\},$$

(23a)

$$\omega_{10} = \frac{\partial}{\partial r} \left(\frac{1}{r} \frac{\partial \psi_{10}}{\partial r} \right),$$

(23b)

$$\frac{\partial \psi_{10}}{\partial r} = 0, \psi_{10} = 0 \text{ at } r = S(z),$$

(23c)

$$\psi_{10} = 0, \frac{\partial \psi_{10}}{\partial z} = 0, \frac{\partial}{\partial r} \left(\frac{1}{r} \frac{\partial \psi_{10}}{\partial r} \right) = 0 \text{ as } r \rightarrow 0,$$

(23d)

$$\text{where } R_{e1} = \frac{R_e}{1+b^{-1}}.$$

First order oscillatory part:

$$D^2 \omega_{11} - \alpha_1^2 \omega_{11} = R_{e1} \left[\frac{1}{r} \left(\frac{\partial \psi_{00}}{\partial r} \frac{\partial \omega_{01}}{\partial z} + \frac{\partial \psi_{01}}{\partial r} \frac{\partial \omega_{00}}{\partial z} \right) - \left\{ \frac{\partial \psi_{01}}{\partial z} \frac{\partial}{\partial r} \left(\frac{\omega_{00}}{r} \right) + \frac{\partial \psi_{00}}{\partial z} \frac{\partial}{\partial r} \left(\frac{\omega_{01}}{r} \right) + M \right\} \right],$$

(24a)

$$\omega_{11} = \frac{\partial}{\partial r} \left(\frac{1}{r} \frac{\partial \psi_{11}}{\partial r} \right),$$

(24b)

$$\frac{\partial \psi_{11}}{\partial r} = 0, \psi_{11} = 0 \text{ at } r = S(z),$$

(24c)

$$\psi_{11} = 0, \frac{\partial \psi_{11}}{\partial z} = 0, \frac{\partial}{\partial r} \left(\frac{1}{r} \frac{\partial \psi_{11}}{\partial r} \right) = 0 \text{ as } r \rightarrow 0.$$

(24d)

The equations (21a,b) and (22a,b) are solved along with the corresponding boundary conditions to give the zeros order of ω and ψ as:

$$\omega_{00} = -\frac{8}{S^4} \{1 - \nu_s F(z)\} r,$$

(25)

$$\psi_{00} = \frac{1}{S^4} \{1 - \nu_s F(z)\} \left\{ 2r^2 (S^2 + g_0 \mu_0) - r^4 - 2S^2 g_0 \mu_0 \right\}$$

(26)

$$\omega_{01} = -2\alpha_1 \{1 - \nu_s F(z)\} \frac{I_1(\alpha_1 r)}{S^2 I_2(\alpha_1 S)},$$

(27)

$$\psi_{01} = \{1 - \nu_s F(z)\} \left[\alpha_1 r I_0(\alpha_1 S) - 2I_1(\alpha_1 r) \right] \frac{r}{\alpha_1 S^2 I_2(\alpha_1 S)},$$

(28)

$$\text{where } g_0 = \frac{S^4}{4\{1 - \nu_s F(z)\}}, I_0(x), I_1(x), I_2(x) \text{ are}$$

modified Bessel functions of order 0, 1, 2 respectively.

Using (25) to (28), we solve equations (23) and (24) for the first order components of ω and ψ .

Then the results are obtained as

$$\omega_{10} = -2 \frac{R_{e1}}{S^8} \{1 - \nu_s F(z)\} (g_1 + 4g_2) \left\{ \left(S^2 + \frac{3}{2} g_0 \mu_0 \right) r S^2 - 2(S^2 + g_0 \mu_0) r^3 + \frac{2}{3} r^5 \right\},$$

(29)

$$\psi_{10} = \frac{1}{36 S^8} \{1 - \nu_s F(z)\} (g_1 + 4g_2) \left\{ 4S^2 + 9g_0 \mu_0 \right\} r^2 S^4 - 9 \left(S^2 + \frac{3}{2} g_0 \mu_0 \right) r^4 S^2$$

$$\left\{ \frac{16(S^2 + g_0 \mu_0)^6}{30r} - r^8 - \frac{3}{2} g_0 \mu_0 S^6 \right\},$$

$$\omega_{11} = \frac{R_{e1}}{\alpha_1^2 S^9 I_2(\alpha_1 S)} \{1 - \nu_s F(z)\} \left\{ T_1 r I_0(\alpha_1 r) - T_2 r^2 I_1(\alpha_1 r) - T_3 r^3 I_2(\alpha_1 r) + T_4 r^4 I_1(\alpha_1 r) - 8T_6 r + T_7 I_1(\alpha_1 r) \right\},$$

(31)

$$\psi_{11} = \frac{R_{e1}}{\alpha_1^4 S^9 I_2(\alpha_1 S)} \{1 - \nu_s F(z)\} \left\{ T_1 r^2 I_2(\alpha_1 r) - T_2 r^3 I_3(\alpha_1 r) - T_3 r^4 I_4(\alpha_1 r) + T_4 r^5 I_3(\alpha_1 r) - \alpha_1^2 T_6 r^4 - T_7 r I_1(\alpha_1 r) - T_8 r^2 \right\},$$

4. Wall Shear Stress

The tangential force per unit area that blood flowing through an artery or biomedical device exerts on its surface is known as wall shear stress, or WSS. It is a crucial hemodynamic metric for comprehending the mechanical relationship between blood flow and the endothelial cells that line the blood vessels. Wall shear stress variations have a major impact on blood circulation, vascular function, and the development of pulmonary and cardiovascular disorders. Specifically, aberrant WSS distribution is linked to flow resistance, vascular dysfunction, and

clinical diseases including pulmonary edema. The shear tension on the wall is provided by

$$\tau'_w = \frac{\left[\sigma_{zr} \left\{ 1 - \left(\frac{dR}{dz} \right)^2 \right\} + (\sigma_{rr} - \sigma_{zz}) \frac{dR}{dz} \right]}{\left\{ 1 + \left(\frac{dR}{dz} \right)^2 \right\}}$$

where $\sigma_r = \mu \left(\frac{\partial w}{\partial r} + \frac{\partial u}{\partial z} \right)$ and $\sigma_r - \sigma_z = -2\mu \left(\frac{\partial w}{\partial z} - \frac{\partial u}{\partial r} \right)$ are calculated at $r = R(z)$.

Then using the boundary conditions at $r = S(z)$ and equations (9) and (11), we obtain the dimensionless wall shear stress τ_w in the following form

$$\begin{aligned} \tau_w &= \frac{2\pi R_0^3}{\mu Q_s} \tau'_w \\ &= (\omega_{00} + \delta e^{it} \omega_{01}) + \varepsilon (\omega_{10} + \delta e^{it} \omega_{11}) + o(\varepsilon^2, \delta^2) \text{ at } r = S(z). \\ &= -\frac{8\{1 - v_s F(z)\}}{S^3} \left[1 + \delta e^{it} \left(\frac{\alpha_1 S I_1(\alpha_1 S)}{4 I_2(\alpha_1 S)} \right) - \varepsilon R_{e1} \left\{ \frac{(g_1 + 4g_2)}{24 S^2} (2S \right. \right. \\ &\quad \left. \left. - \frac{\delta e^{it}}{8 \alpha_1^2 S^6 I_2(\alpha_1 S)} \{ M + T_1 S I_0(\alpha_1 S) - T_2 S^2 I_1(\alpha_1 S) - T_3 S^3 I_2(\alpha_1 S) \right. \right. \\ &\quad \left. \left. + o(\varepsilon^2, \delta^2) \right\} \right] \end{aligned}$$

5. Results and Discussions

Because of the magnetic field effects and the pulsatile character of the blood flow, the resulting expressions require complex parameters. However, only the genuine portions of these expressions are taken into account for computational analysis and physical interpretation. Plotting the axial coordinate (z) against the relevant flow characteristics allows one to examine the hemodynamic behavior linked to pulmonary edema disease.

The stream function variation along the axial direction (z) for blood flow through a non-uniform circular tube under wall suction circumstances is depicted in Figure 5. The graphical depiction illustrates how the pulmonary artery's flow circulation is impacted by vessel shape and magnetic field strength. The variation of wall shear stress (WSS) in relation to the axial coordinate (z) is shown in Figure 6. The findings show that variations in arterial irregularities and magnetic field intensity have a major impact on the distribution of shear stress along the artery wall, which is crucial for comprehending

endothelial dysfunction and vascular resistance in pulmonary edema.

Graphical analysis is also used to examine how various flow factors affect the dimensionless pressure drop (delta). For a sinusoidal tube with wall injection at Hartmann number (M = 2), Figure 7 shows the pressure gradient vs (z). Because of the Lorentz force, the magnetic field increases flow resistance and lowers axial velocity, which causes observable changes in the blood flow's pressure characteristics.

These computational discoveries may help to better understand pulmonary artery flow under magnetic field effects and offer significant insights into the intricate hemodynamics of pulmonary edema.

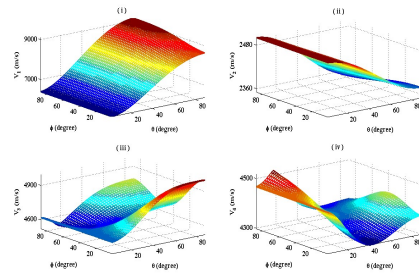


Fig 5. Wall shear stress and velocity gradient in blood flow in artery in presence of pulmonary edima and M=2.

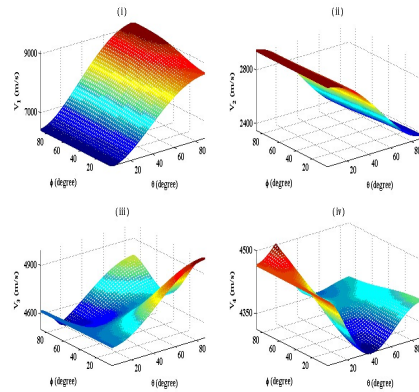


Fig 6. Wall shear stress and velocity gradient for M=2.

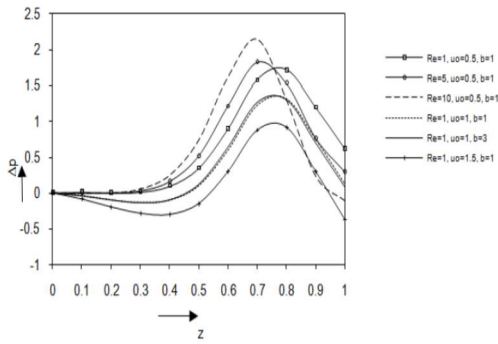


Fig.7 Pressure gradient vs z for sinusoidal tube with injection at the $M=1$

6. Conclusion

The pulsatile magneto hydrodynamic (MHD) blood flow via a non-uniform circular tube with slip velocity, suction, and injection effects is examined in this computational work, with a focus on pulmonary edema disease. The analysis shows that the slip parameter, tube shape, and magnetic field have a significant impact on the hemodynamic properties of blood flow. The findings show that because there is less frictional resistance at the artery wall when the slip parameter rises, the pressure drop dramatically lowers.

The study also demonstrates that the Hartmann number, which represents the strength of the magnetic field, has a significant impact on the velocity distribution and wall shear stress. Because of the resistive Lorentz force created by the interaction between the magnetic field and electrically conducting blood, an increase in the Hartmann number decreases the axial velocity. As a result, the non-uniform pulmonary artery experiences increased flow resistance and pressure fluctuations. In pulmonary edema, excess fluid accumulation in the lungs changes pulmonary circulation and raises vascular resistance; these consequences are especially significant.

Additionally, a thorough understanding of blood flow behavior in capillaries and small blood vessels—where suction, injection, and slip velocity effects become important at low Reynolds numbers—is provided by the computational approach. Because aberrant shear stress distribution may lead to endothelial dysfunction and decreased pulmonary blood circulation associated with pulmonary edema

disease, the differences in wall shear stress seen in this model are physiologically significant.

The study further emphasizes the importance of magnetic field-assisted blood flow control for biomedicine. The design and optimization of biomedical equipment, including blood pumps, arterial stents, magnetic drug targeting systems, and other therapeutic technologies, benefit from an understanding of how magnetic fields and artery geometry affect blood circulation. Thus, the current model may help develop better methods for diagnosing and treating pulmonary edema and associated cardiovascular conditions.

In the future, the study can be expanded by taking into account elastic artery walls, heat transfer effects, non-Newtonian blood behavior, and sophisticated computational simulations for more physiological situations.

References

1. Womersley, JR., Method for the calculation of velocity, rate of flow and viscous drag in arteries when the pressure gradient is known, *J. physiol.*, **127** (1955) 553-563.
2. Kumar, Anil, Varshney C. L. and Sharma G.C. (2005). Computational technique for flow in blood vessels with porous effects. *Applied Mathematics and Mechanics*, **26**, 63-72.
3. R. K. Saket and Anil Kumar(2008): Reliability of convective diffusion process in porous blood vessels, *Chemical Product and Process Modeling*, Vol.(3) Article (25) ISSN: 1934-2659, Canada 2008, Anil Kumar, C L Varshney and GC Sharma (2005): Performance modeling and analysis of blood flow in elastic arteries, *Applied Mathematics and Mechanics*, **26**(3) ,pp 345–354(2005)Schneck, DJ., Ostrach, S., Pulsatile blood flow in a channel of small exponential divergence-I. The linear approximation for low mean Reynolds number, *J. Fluids Eng.*, **16** (1975) 353-360.
4. Bitoun, JP., Bellet, D., Blood flow through a stenosis in micro-circulation, *Biorheology*, **23** (1986) 51-61.
5. Manton, MJ., “ Low Reynolds number flow in slowly varying axisymmetric tubes”, *J. Fluid Mech.*, **49** (1971) 451-459.

6. Radhakrishnamacharya, G., Chandra, P., Kaimal, MR., "A hydro dynamical study of flow in renal tubule", *Bull. Math. Biol.*, **43** (1981) 151-163.
7. Chandra, P., Prasad, JS., "Pulsatile flow in circular tubes of varying cross-section with suction/injunction", *J. Austral. Math. Soc.*, **35** (1994) 336-381.
8. Chow, JCF. Blood flow theory, effective viscosity and effects of particle distribution", *Bull. Math. Biol.*, **37** (1975) 472-488.
9. Hill, CD., Bedford, A., "A model for erythrocyte sedimentation", *Biorheology*, **18** (1981) 255.
10. Srivastava, LM., Agarwal, RP., "Oscillating flow of a conducting fluid with a suspension of spherical particles", *J. Appl. Mech.*, **47** (1980) 196.
11. Nakayama, M., Sawada, TJ., "Numerical study on the flow of a non-Newtonian fluid through an axisymmetric stenosis", *Biomech. Eng.*, **110** (1988) 137.
12. Elnaby, MA., Eldabe, NT M., Abou Zied, MY., Sanyal, DC., Mathematical analysis on MHD. pulsatile flow of a non-Newtonian fluid through a tube with varying cross-section", *J. of Inst. of Math. and Comp. Sci.*, **20** (2007) 29-42.
13. Sanyal, DC., Das, K., Debnath, S., "Pulsatile flow of biviscous fluid through a tube of varying cross-section", *International Journal of computational Intelligence and Healthcare Informatics*, **1** (2008) 1-8.
14. Stroud, J.S.; Berger, S.A. and Saloner, D. (2000). Influence of stenosis morphology on flow through severely stenotic vessels: implications for plaque rupture, *J. Biomechanics*, **33**, 443-455.
15. Sharma, G.C.; Jain, M. and Kumar, Anil (2001). Finite element Galerkin approach for a computational study of arterial flow, *Applied Mathematics and Mechanics*, **22**, 1012-1018.
16. Anil Kumar and SP Agrawal (2014): Computational study of blood flow through elastic arteries with porous effects, 3rd Soft Computing for problem solving (Soc Pros 2013) organized by Indian Institute of Technology Roorkee, 2013 Advances in Intelligent Systems and Computing published Proceedings Springer publishing, vol. 1 pp 1-10, 2014
17. Shit, G. C. Computational Modelling publication Modelling and Simulation in Engineering, 7th edition, pp 15-26, 2013.
18. Anil Kumar, Mathematical study of blood flow in a circular tube of varying cross-section of non-Newtonian biviscous incompressible fluid in the permeable wall. *Biomedical Science and Engineering*, vol. 5, no. 1 (2017): 1-4. doi: 10.12691/bse-5-1-1.
19. Anil Kumar and SP Agrawal (2014): Computational study of blood flow through elastic arteries with porous effects, 3rd Soft Computing for problem solving (Soc Pros 2013) organized by Indian Institute of Technology Roorkee, 2013 [Advances in Intelligent Systems and Computing](#) published Proceeding Springer publishing, vol. 1 pp 1-10, 2014.
20. Anil Kumar and S P Agarwal (2015): Computer Modeling and analysis of the hydrodynamic parameters of blood flow through stenotic artery, Third International Conference on Recent Trends in Computing , India Procedia Computer Science, Elsevier publication, **57** (2015) 403 – 410.
21. Anil Kumar Gupta (2009): Finite Element Galerkin's scheme for flow in blood vessels with magnetic effects, *International Journal of Applied Systemic Studies*, vol. 2 (3) pp- 284-293.
22. Anil Kumar Gupta (2011): Performance and analysis of blood flow through carotid artery, *International Journal of Engineering and Business Management* Vol. 3, No. 4, pp 1-6.
23. Anil Kumar Gupta (2011): Performance Model and Analysis of Blood Flow in Small Vessels with Magnetic Effects, *International Journal of Engineering, IJE Transactions A: Basics*, Vol. 25, No. 2, pp 190 -196.
24. Anil Kumar :Modeling of blood flow through elastic arteries and their applications, Proceedings on 09th INDIACom, 2nd International Conference on Computing for Sustainable Global Development, 11-13 March 2015 , IEEE Bharti Vidyapeeth New Delhi ISSN 0973-7529; ISBN 978-93-80544-15-1 pp 89-94. **Scopus Index** 04 May 2015 <https://ieeexplore.ieee.org/document/7100395>

Computational Modeling of Blood Flow in a Non-Uniform Circular Tube under Magnetic Field effects
with Application to Pulmonary Edema Disease

25. Anil Kumar, Gaurav Varshney, and Akash: Modeling and Analysis of Blood Movement in Stenosis vessels under the Stimulus of Permeability and Magnetization Parameters, *Utilitas Mathematica* vol. 122, pp 698-705, 2025
- 26.